

Single cell RNA-sequencing analysis reveals that *N*-acetylcysteine partially reverses hepatic immune dysfunction in biliary atresia

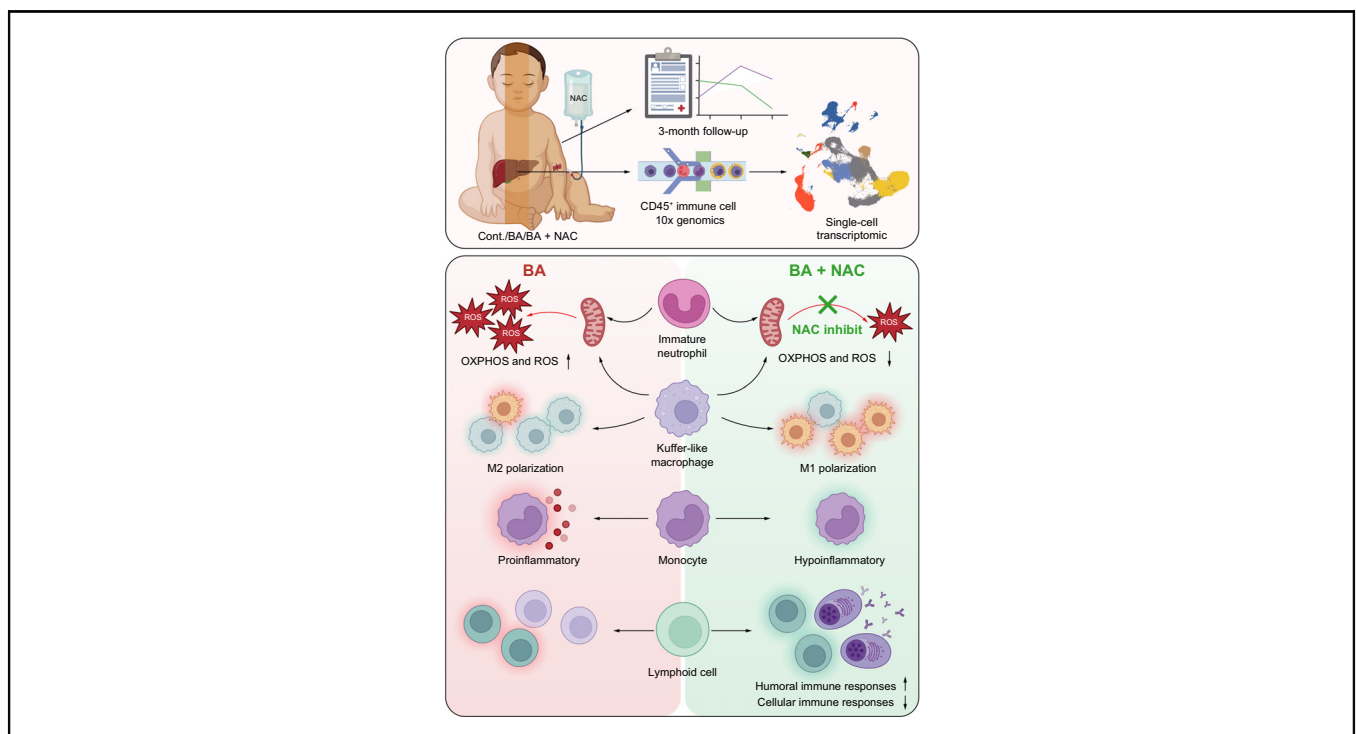
Authors

Rongchen Ye, Sige Ma, Yan Chen, Jiarou Shan, Ledong Tan, Liang Su, Yanlu Tong, Ziyang Zhao, Hongjiao Chen, Ming Fu, Zhipeng Guo, Xiaoyu Zuo, Jiakang Yu, Wei Zhong, Jixiao Zeng, Fei Liu, Chenwei Chai, Xisi Guan, Zhe Wang, Tao Liu, Jiankun Liang, Yan Zhang, Hongguang Shi, Zhe Wen, Huimin Xia, Ruizhong Zhang

Correspondence

zhangruizhong@gwcmc.org (R. Zhang), xia-huimin@foxmail.com (H. Xia), wenzhe2005@163.com (Z. Wen).

Graphical abstract



Highlights

- Intravenous NAC treatment improves bilirubin metabolism and bile acid flow in patients with BA.
- NAC suppresses CD177⁺ hepatic immature neutrophil oxidative phosphorylation and reactive oxygen species production in BA.
- NAC alleviates monocyte-mediated inflammation and reverses hepatic macrophage dysfunction in BA.
- NAC downregulates innate/adaptive proinflammatory responses via cell–cell interactions in BA.

Impact and implications

BA is a serious liver disease that affects newborns and has no effective drug treatment. In this study, scRNA-seq showed that NAC treatment can partially reverse the immune dysfunction of neutrophil extracellular trap-releasing CD177⁺ neutrophils and Kupffer cells, and lower the inflammatory responses of other innate immune cells in BA. In consequence, intravenous NAC treatment improved the clinical outcomes of patients with BA in term of bilirubin metabolism.

Single cell RNA-sequencing analysis reveals that *N*-acetylcysteine partially reverses hepatic immune dysfunction in biliary atresia



Rongchen Ye,^{1,†} Sige Ma,^{1,†} Yan Chen,^{2,1,†} Jiarou Shan,¹ Ledong Tan,¹ Liang Su,¹ Yanlu Tong,¹ Ziyang Zhao,¹ Hongjiao Chen,¹ Ming Fu,¹ Zhipeng Guo,¹ Xiaoyu Zuo,¹ Jiakang Yu,¹ Wei Zhong,¹ Jixiao Zeng,¹ Fei Liu,¹ Chenwei Chai,¹ Xisi Guan,¹ Zhe Wang,¹ Tao Liu,¹ Jiankun Liang,¹ Yan Zhang,¹ Hongguang Shi,³ Zhe Wen,^{1,*} Huimin Xia,^{1,*} Ruizhong Zhang^{1,3,*}

¹Guangdong Provincial Key Laboratory of Research in Structure Birth Defect Disease and Department of Pediatric Surgery, Guangzhou Women and Children's Medical Center, Guangzhou Medical University, Guangdong Provincial Clinical Research Center for Child Health, Guangzhou, 510623, China; ²Faculty of Medicine, Macau University of Science and Technology, Macau, 999078, China; ³Department of Pediatric Surgery, The Third Affiliated Hospital of Zhengzhou University, Zhengzhou, 450052, China

JHEP Reports 2023. <https://doi.org/10.1016/j.jhepr.2023.100908>

Background & Aims: Our previous study indicated that CD177⁺ neutrophil activation has a vital role in the pathogenesis of biliary atresia (BA), which is partially ameliorated by *N*-acetylcysteine (NAC) treatment. Here, we evaluated the clinical efficacy of NAC treatment and profiled liver-resident immune cells via single cell RNA-sequencing (scRNA-seq) analysis to provide a comprehensive immune landscape of NAC-derived immune regulation.

Methods: A pilot clinical study was conducted to evaluate the potential effects of intravenous NAC treatment on infants with BA, and a 3-month follow-up was carried out to assess treatment efficacy. scRNA-seq analysis of liver CD45⁺ immune cells in the control (n = 4), BA (n = 6), and BA + NAC (n = 6) groups was performed and the effects on innate cells, including neutrophil and monocyte-macrophage subsets, and lymphoid cells were evaluated.

Results: Intravenous NAC treatment demonstrated beneficial efficacy for infants with BA by improving bilirubin metabolism and bile acid flow. Two hepatic neutrophil subsets of innate cells were identified by scRNA-seq analysis. NAC treatment suppressed oxidative phosphorylation and reactive oxygen species production in immature neutrophils, which were transcriptionally and functionally similar to CD177⁺ neutrophils. We also observed the suppression of hepatic monocyte-mediated inflammation, decreased levels of oxidative phosphorylation, and M1 polarisation in Kupffer-like macrophages by NAC. In lymphoid cells, enhancement of humoral immune responses and attenuation of cellular immune responses were observed after NAC treatment. Moreover, cell-cell interaction analysis showed that innate/adaptive proinflammatory responses were downregulated by NAC.

Conclusions: Our clinical and scRNA-seq data demonstrated that intravenous NAC treatment partially reversed liver immune dysfunction, alleviated the proinflammatory responses in BA by targeting innate cells, and exhibited beneficial clinical efficacy.

Impact and implications: BA is a serious liver disease that affects newborns and has no effective drug treatment. In this study, scRNA-seq showed that NAC treatment can partially reverse the immune dysfunction of neutrophil extracellular trap-releasing CD177⁺ neutrophils and Kupffer cells, and lower the inflammatory responses of other innate immune cells in BA. In consequence, intravenous NAC treatment improved the clinical outcomes of patients with BA in term of bilirubin metabolism. © 2023 The Authors. Published by Elsevier B.V. on behalf of European Association for the Study of the Liver (EASL). This is an open access article under the CC BY-NC-ND license (<http://creativecommons.org/licenses/by-nc-nd/4.0/>).

Introduction

Biliary atresia (BA) is a progressive neonatal cholangiopathy with poor prognosis and high mortality that is characterised by

extrahepatic bile duct obstruction-induced pathological jaundice, liver fibrosis, and liver failure. To date, surgery is the main option for BA treatment given that pharmacotherapy for this condition is lacking. However, there are numerous clinical trials testing repurposed therapeutics, including corticosteroid,¹ intravenous immunoglobulin,² odevixibat,³ and colony-stimulating factor.⁴ It was recently reported that rituximab (anti-CD20), a B cell-modifying therapy, promotes immune recovery in infants with BA.⁵

N-acetylcysteine (NAC) is a cysteine precursor that has been used to reduce the severity of liver injury caused by acetaminophen overdose,⁶ as well as to treat non-acetaminophen-induced acute liver failure in children.⁷ Our recent study also

Keywords: scRNA-seq; Biliary atresia; *N*-acetylcysteine; Innate immune response; Neutrophil; Oxidative phosphorylation.

Received 19 January 2023; received in revised form 12 July 2023; accepted 22 August 2023; available online 12 September 2023

† Co-first authors.

* Corresponding author. Address: Guangdong Provincial Key Laboratory of Research in Structure Birth Defect Disease, Guangzhou Women and Children's Medical Center, Guangzhou Medical University, No. 9, Jinshui Road, Guangzhou, 510623, Guangdong, China. Tel: 020-38076560; fax: 020-38076560.

E-mail addresses: zhangruizhong@gwcmc.org (R. Zhang), xia-huimin@foxmail.com (H. Xia), wenzhe2005@163.com (Z. Wen).



ELSEVIER

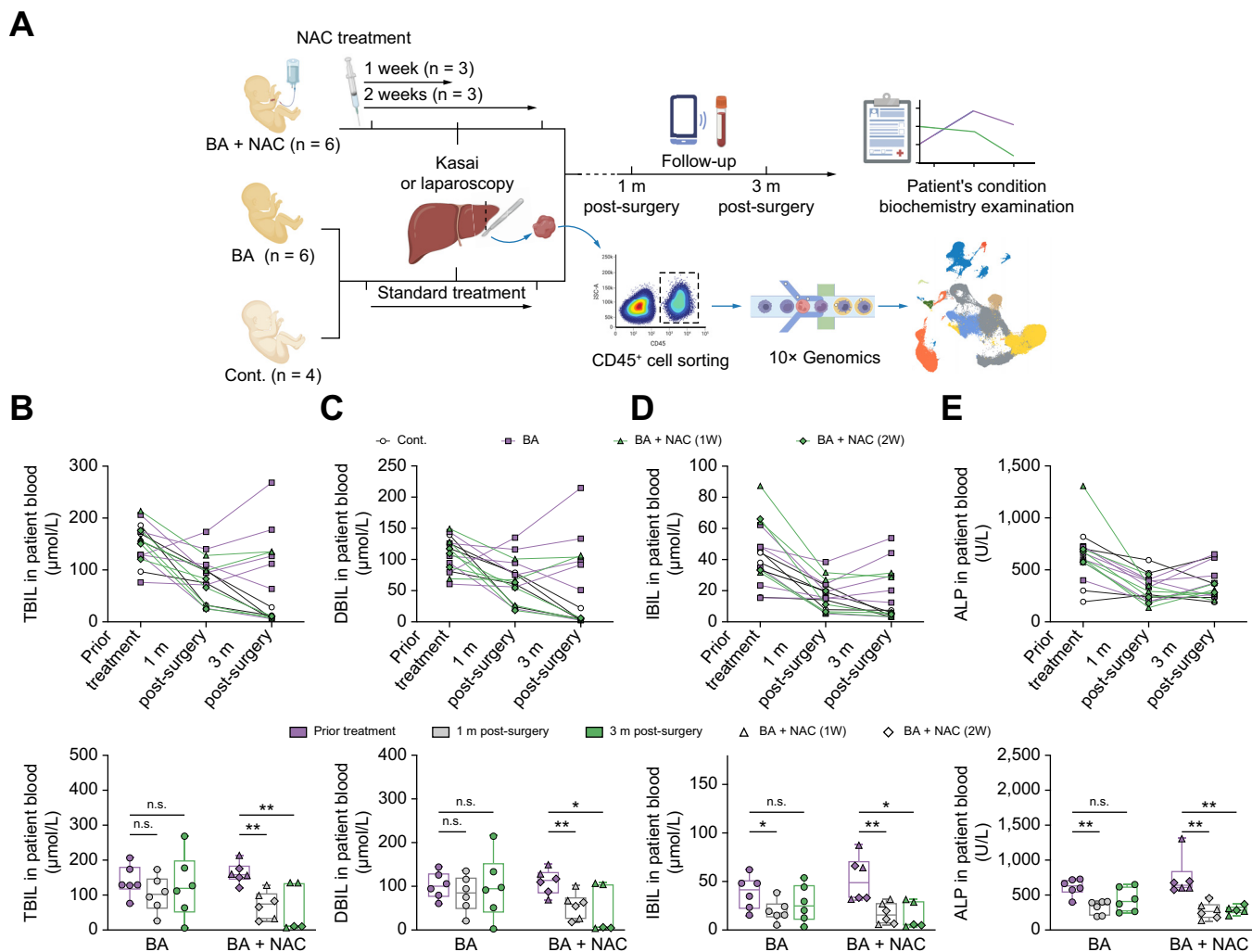


Fig. 1. Biochemical changes in infants with BA 3 months after Kasai surgery. (A) Overview depicting the workflow of this study. (B–E) Levels of (B) TBIL, (C) DBIL, (D) IBIL, and (E) ALP over time. In all treatment groups n = 6 (prior BA treatment; BA+NAC prior treatment; BA 1 month post-surgery; BA+NAC 1 month post-surgery; and BA 3 months post-surgery) except BA+NAC 3 months post-surgery (n = 5). Data are mean ± SD, analysed with Student 2-tailed *t* test; **p* ≤ 0.05; ***p* ≤ 0.01. ALP, alkaline phosphatase; BA, biliary atresia; Cont., control; DBIL, direct bilirubin; IBIL, indirect bilirubin; NAC, *N*-acetylcysteine; TBIL, total bilirubin.

showed that NAC treatment significantly ameliorated pathology by reducing oxidative phosphorylation (OXPHOS) and reactive oxygen species (ROS) levels, which have a crucial role in biliary epithelial cell (BEC) damage in both patients with BA and animal models.^{8,9} However, the mechanism by which NAC treatment alters liver immune regulation at single cell resolution in infants with BA remains unexplored.

As part of our clinical trial, a 3-month clinical follow-up of infants receiving NAC treatment after Kasai surgery was performed. Additionally, we profiled the single cell transcriptomes of 168,577 liver-resident immune cells (CD45⁺ cells) from liver biopsies. The interactions between cell types were also determined. Our data provide evidence that NAC partially reverses liver immune dysfunction and alleviates proinflammatory responses in BA by targeting innate cells and, thus, could be used in the clinical setting in infants with BA;

however, large-scale clinical trials are needed to investigate this further.

Patients and methods

Ethics statement and biopsy collection

The Medical Ethics Committee of Guangzhou Women and Children's Medical Center approved the study procedures and clinical trial (ID: 62001). The clinical trial was registered with the Chinese Clinical Trial Registry (ChiCTR2000040505). The implementations were in concordance with the International Ethical Guidelines for Research Involving Human Subjects as stated in the Helsinki Declaration. The legal guardians of all participants signed consent forms. Liver biopsies were obtained during Kasai surgery or laparoscopy from 16 patients enrolled in the clinical

trial. The details of the patients and methods are provided in the supplementary material online.

Results

Clinical efficacy of NAC treatment for infants with BA

Given that our previous study found that intravenous NAC can ameliorate the pathological condition of BA,⁸ we primarily focussed here on the clinical efficacy of NAC treatment for infants

with BA by carrying out a 3-month follow-up to evaluate the condition and biochemical examination changes in these participants (Fig. 1A).

Follow-up data showed that the levels of total bilirubin (TBIL), direct bilirubin (DBIL), indirect bilirubin (IBIL), and alkaline phosphatase (ALP), which can indicate cholestasis, were significantly ameliorated in the BA+NAC group at both 1 and 3 months post-surgery compared with those before treatment, whereas there were no significant improvements in the BA group

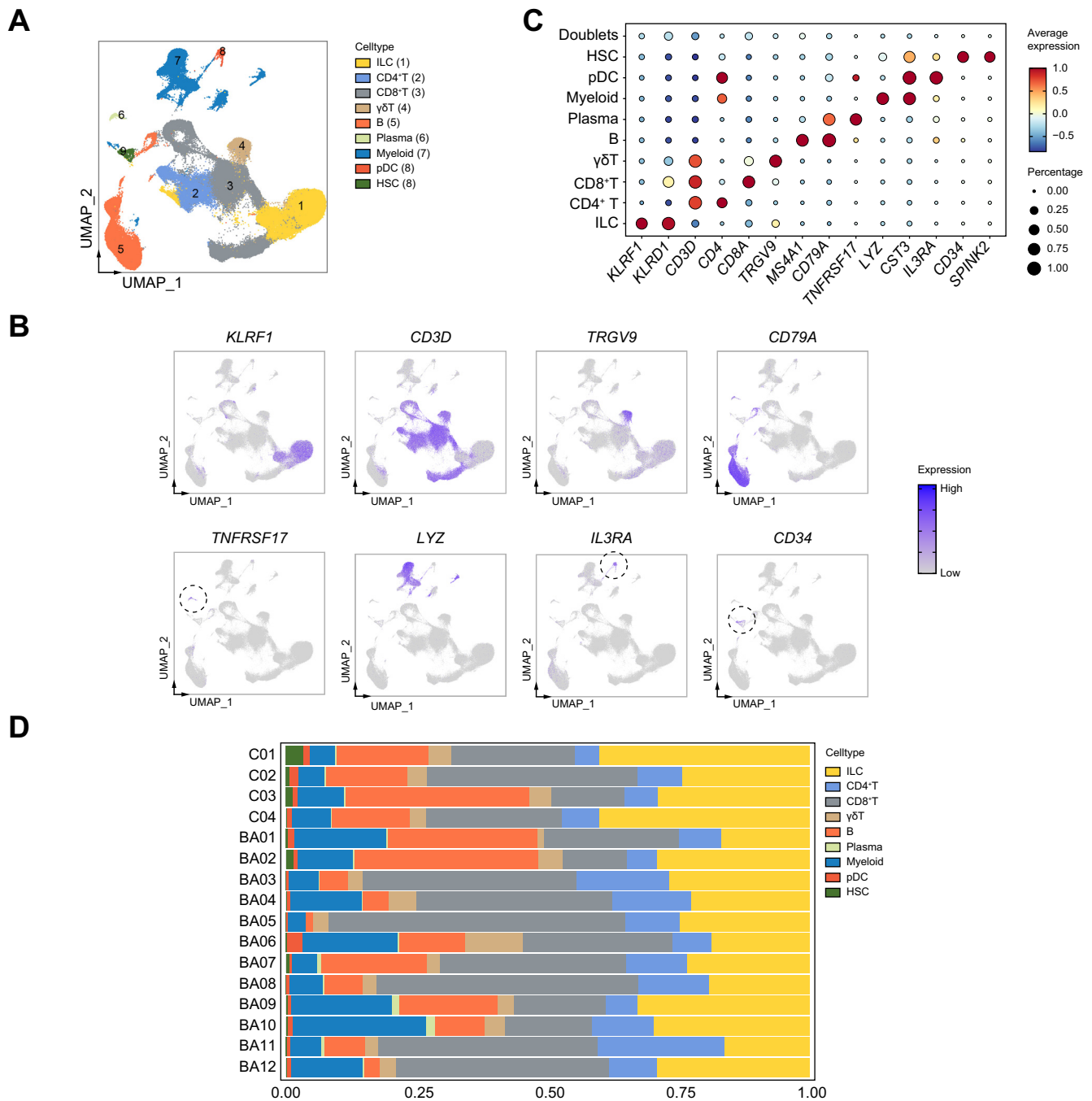


Fig. 2. scRNA-seq atlas of liver immune cells. (A) UMAP plot showing 168,577 cells representing nine liver immune cell types, coloured by cell type. (B) UMAP plots displaying marker gene expressions for each immune cell type. (C) Bubble heatmap showing marker gene expressions across immune cell types. (D) Distributions of nine liver immune cell types across batches. HSC, haematopoietic stem cell; ILC, innate lymphoid cell; pDC, plasmacytoid dendritic cell; scRNA-seq, single cell RNA-sequencing; UMAP, uniform manifold approximation and projection.

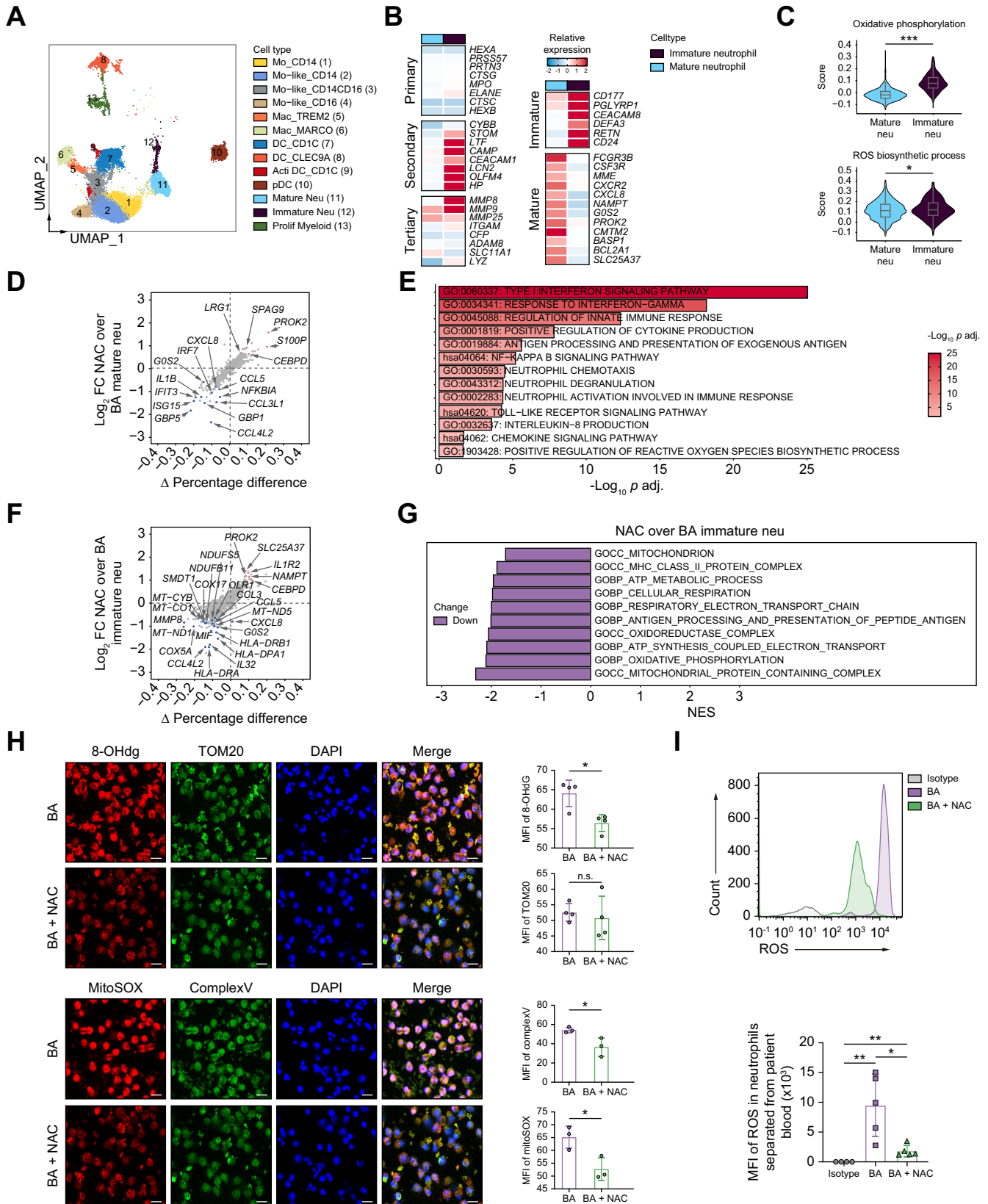


Fig. 3. Decreased OXPHOS in hepatic immature neutrophils following NAC treatment. (A) UMAP plot showing 17,958 cells of 12 myeloid subsets, coloured by cell type. (B) Heatmap of the expression of marker genes and neutrophil granule proteins representing mature neutrophils and immature neutrophils. (C) OXPHOS and ROS biosynthesis process scores in mature and immature neutrophils. (D) Comparison of DEGs for mature neutrophils between the BA+NAC and BA groups. (E) Enriched GO terms and KEGG pathways of the genes downregulated in the BA+NAC group compared with the BA group for mature neutrophils. Colour

(without NAC treatment) (Fig. 1B–E). Although Kasai surgery improves bilirubin metabolism and bile acid flow, these surgical effects are not maintained in the long run; nevertheless, they were enhanced by NAC treatment. However, the three patients who received NAC treatment for an additional week post-surgery did not show significant improvement compared with three patients who only received NAC treatment for 1 week.

In addition, other parameters representing liver function and the onset of post-surgical complications in the BA+NAC group were not significantly different from those in the BA group post-surgery, suggesting that NAC does not improve liver function (Fig. S1A–D; Table S1). These results showed that NAC treatment can ameliorate cholestasis and improve bile flow, suggesting partial beneficial clinical efficacy of NAC treatment for infants with BA.

Single cell transcriptomic landscape of liver immune cells

To fully understand the potential mechanism of clinical efficacy, we conducted a comprehensive investigation of BA liver immune regulation by NAC treatment at the single cell resolution. Liver immune cells (CD45⁺ cells) from patients were isolated and scRNA-seq analysis was performed using the 10X platform (Fig. 1A). The raw off-machine sequencing data were pre-processed by Cell Ranger. For downstream analysis, Seurat was applied to process the raw unique molecular identifier (UMI) count matrix. After data preprocessing and rigorous quality control definition, low-quality cells, defined as those with a high number of genes and UMIs and abnormal proportions of mitochondrial and erythrocyte RNA, were filtered out. This resulted in 168,577 high-quality transcriptomes from liver immune cells (Fig. S2A–D and Table S2). To identify the heterogeneity and remove batch effects, the Harmony algorithm was applied to integrate the transcriptomes, enabling analysis of a total of 168,577 batch effect-corrected cells (Fig. S3A,B). The batch effect-corrected gene expression matrix was clustered into 35 clusters and nine major cell types with an abnormal subset (Doublets), which were visualised via the uniform manifold approximation and projection (UMAP) algorithm (Fig. 2A and Fig. S3C). The major cell types were identified based on the expression of known canonical marker genes (Fig. 2B,C). Given the high value of complexity and absence of specific marker genes (details in 'Patients and methods' section), Doublets were identified and removed in further downstream analysis (Fig. 2C and Fig. S3D). The distribution of these major cell types across batches and groups was visualised (Fig. 2D and Fig. S3E). Innate lymphoid cells were relatively heterogeneous between batches; thus, we did not perform any further analysis but focused mainly on the other cell types.

NAC treatment suppressed hepatic immature neutrophil oxidative phosphorylation

Gr-1⁺ cells (comprising Ly6g⁺ and Ly6c⁺) respond to virus infection and mediate bile duct damage in the initiation of mouse BA

model, indicating that they might be the main innate immune cell population;⁸ thus, myeloid cells were examined by further subclustering. They clustered into 12 cell subsets based on the expression of known canonical marker genes, and an abnormal subset (Doublets) was removed from downstream analysis (Fig. 3A and Fig. S4A,B). The distribution of myeloid subsets across groups is shown in Fig. S4C.

Given that hepatic CD177⁺ neutrophils exhibit increased OXPPOS levels and release neutrophil extracellular traps (NETs), which cause BEC apoptosis,⁸ we primarily focused on hepatic neutrophil subsets. According to published markers,^{10,11} we confirmed the status of the two neutrophil subsets by determining the secondary neutrophil granule gene expression (Fig. 3B). The surface marker CD177 was highly expressed in immature neutrophils, suggesting that hepatic immature neutrophils are transcriptionally similar to the CD177⁺ cells previously described.⁸ The functional scores of OXPPOS (Hallmark) and the ROS biosynthetic process [Gene Ontology (GO): 1903409] were both significantly increased in immature neutrophils (Fig. 3C).

To further determine transcriptional and functional differences in these two neutrophil subsets between the BA+NAC and BA groups, differentially expressed gene (DEG) analysis was performed; scatter plots showed that chemokine genes, interferon (IFN)-response genes, and other inflammation-related genes were downregulated in the BA+NAC group, indicating mature neutrophil hypoinflammation after NAC treatment (Fig. 3D and Table S3). Further gene enrichment analysis was applied for the downregulated DEGs, indicating that the proinflammatory function and activation of mature neutrophils might be downregulated in the innate immune responses (Fig. 3E). DEG analysis of immature neutrophils (Table S3) showed that chemokine genes, mitochondria-related genes, respiratory chain-related genes, major histocompatibility complex (MHC) class II antigen-related genes, and inflammation-related genes were downregulated in the BA+NAC group (Fig. 3F). Compared with the control (Cont.) group, these aforementioned genes were downregulated in the BA+NAC group in both mature and immature neutrophils (Fig. S4D and Table S3).

To further understand the effects of NAC on immature neutrophils, gene set enrichment analysis (GSEA) was performed with gene signature sets from GO (Table S4). The significantly downregulated pathways (Fig. 3G) indicated that NAC intervention could suppress OXPPOS via the mitochondrial respiratory electron chain.

To validate the suppression of immature neutrophil respiration and OXPPOS by NAC, we next sorted neutrophils from peripheral blood from patients with BA that had been cultured with or without NAC inhibition. Phenotype analysis confirmed that most neutrophils highly expressed CD66b (Fig. S4E), which matched the hepatic immature neutrophil phenotype. The level of Complex V, an enzyme involved in mitochondrial OXPPOS,

represents the log₁₀-transformed adjusted *p* value. (F) Comparison of DEGs for immature neutrophils between the BA+NAC group and BA group. (G) GSEA of selected enriched GO terms for immature neutrophils in the BA+NAC group compared with the BA group. The length of the bar indicates the enrichment score. Colour represents the log₁₀-transformed *q* value. (H) Representative image of MitoSOX (red) and Complex V (green) and quantification. (I) Representative image of 8-OHdG (red) and TOM20 (green) and quantification. Data analysed with a 2-sided Wilcoxon rank-sum test (C) or Student 2-tailed *t* test (H,I); **p* < 0.05, ***p* < 0.01, ****p* < 0.001. Scale bars: 10 μm. BA, biliary atresia; DEGs, differentially expressed genes; GSEA, gene set enrichment analysis; GO, Gene Ontology; KEGG, Kyoto Encyclopedia of Genes and Genomes; MFI, mean fluorescence intensity; NAC, *N*-acetylcysteine; OXPPOS, oxidative phosphorylation; ROS, reactive oxygen species; UMAP, uniform manifold approximation and projection.

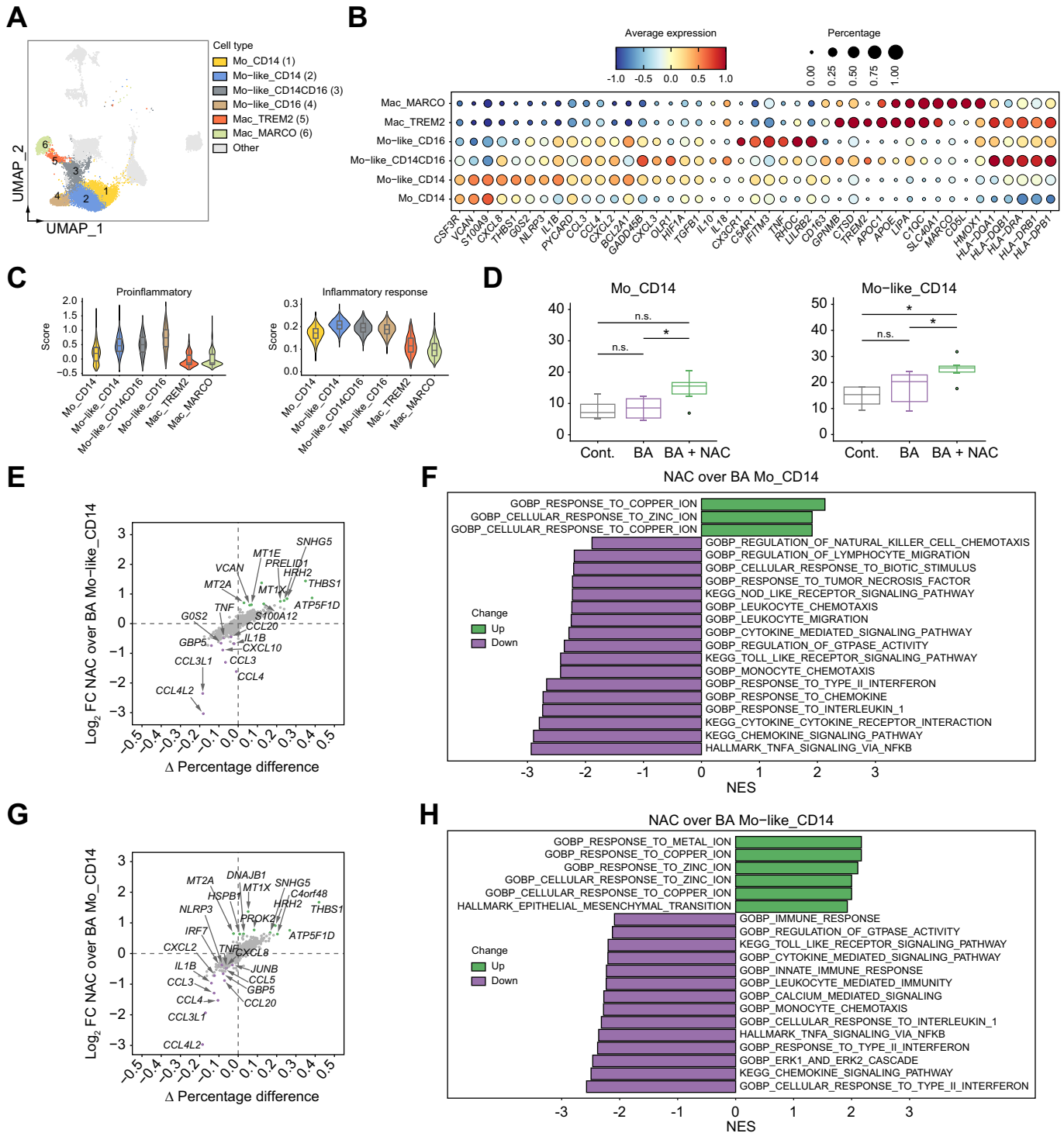


Fig. 4. Hepatic monocyte-mediated inflammation is alleviated by NAC treatment in infants with BA. (A) UMAP plot showing 23,381 cells of monocyte-macrophage subsets, highlighted by cell type. (B) Bubble heatmap showing the gene signatures of monocyte-macrophage subsets. (C) Violin plots showing the proinflammatory and inflammatory response scores of monocyte-macrophage subsets. (D) Proportions of Mo_CD14 and Mo-like_CD14 in myeloid subsets across groups. (E,G) Comparison of DEGs for Mo_CD14 and Mo-like_CD14 between the BA+NAC and BA groups. (F,H) GSEA of selected enriched GO, KEGG, and Hallmark terms for Mo_CD14 and Mo-like_CD14 in the BA+NAC group compared with the BA group. The length of the bar indicates the NES. Colour represents the up- or downregulated terms. Data analysed using a 2-sided Wilcoxon rank-sum test; **p* < 0.05. BA, biliary atresia; cont. control; GO, Gene Ontology; GSEA, gene set enrichment analysis; KEGG, Kyoto Encyclopedia of Genes and Genomes; NAC, N-acetylcysteine; NES, normalised enrichment score.

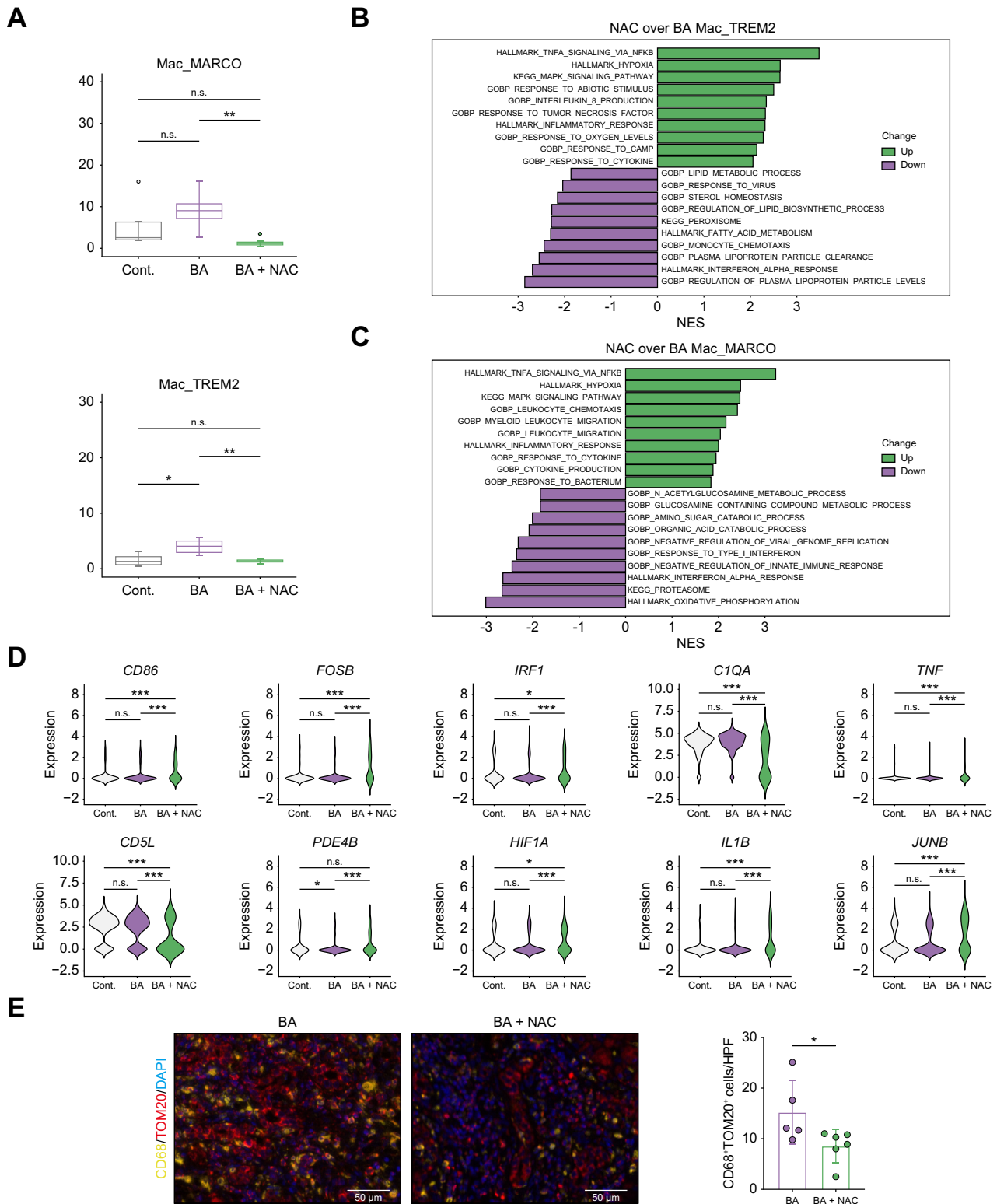


Fig. 5. Hepatic macrophage polarisation with increased phagocytic functions following NAC treatment. (A) Proportions of Mac_TREM2 and Mac_MARCO in myeloid subsets across groups. (B,C) GSEA of selected enriched GO, KEGG, and Hallmark terms for Mac_TREM2 and Mac_MARCO in the BA+NAC group compared with the BA group. The length of the bar indicates the NES. Colour represents the up- or downregulated terms. (D) Expression levels of genes involved in M1-related, proinflammatory, and phagocytic functions. (E) Representative image of TOM20 (red) and CD68 (yellow) in liver slides from BA (n = 5) or BA+NAC (n = 6) groups and quantification. Orange indicates colocalisation. Data analysed using a 2-sided Wilcoxon rank-sum test (A,D) or Student's 2-tailed t test (E); **p* < 0.05, ***p* < 0.01, NS, ****p* < 0.001. Scale bars: 50 μ m. BA, biliary atresia; Cont., control; GSEA, gene set enrichment analysis; NAC, N-acetylcysteine; NES, normalised enrichment score.

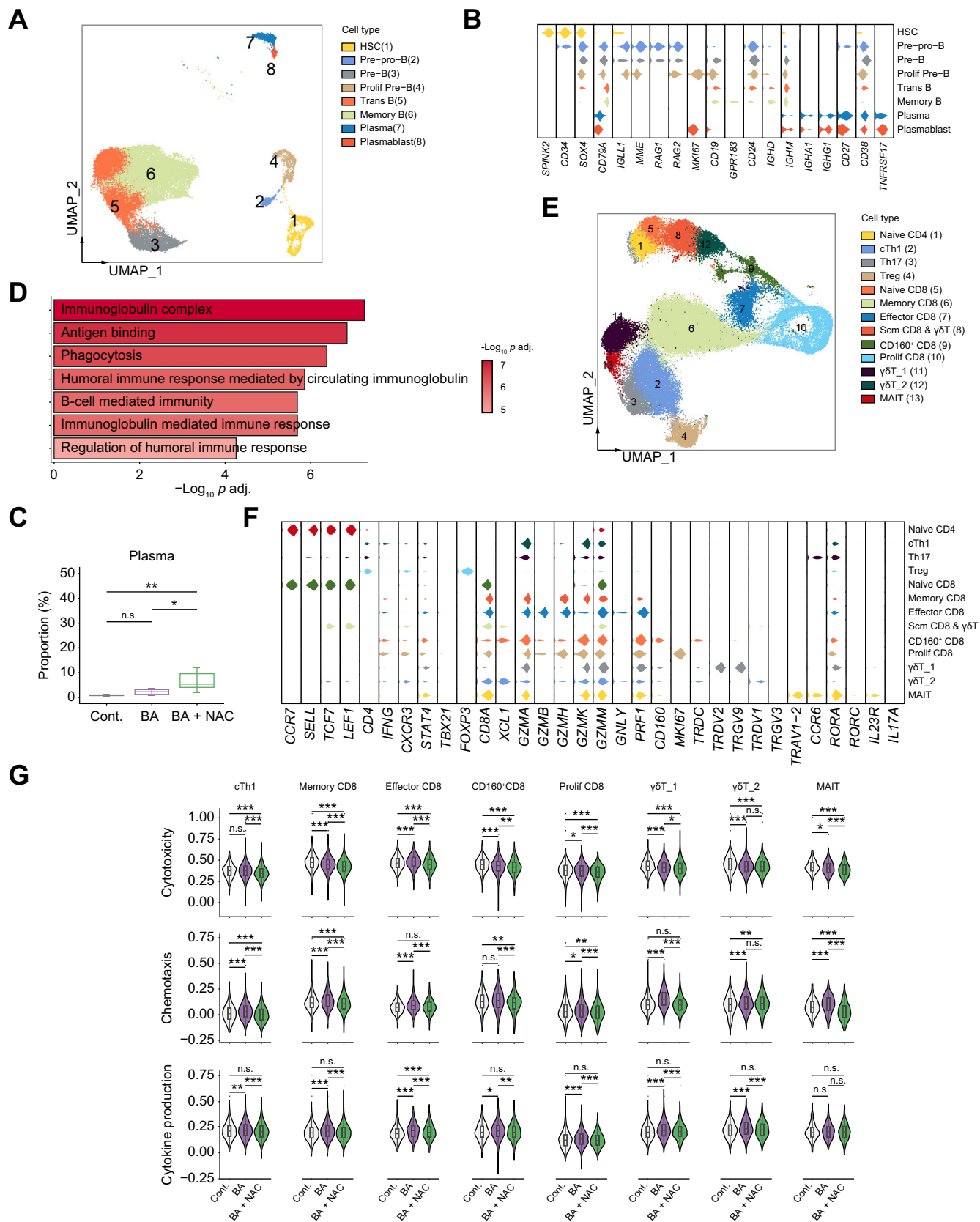


Fig. 6. Analysis of adaptive immune response alterations following NAC treatment. (A) UMAP plot showing 25,716 cells of eight B cell subsets, coloured by cell type. (B) Canonical marker gene expression across B cell subsets. (C) Proportions of plasma in B cell subsets across groups. (D) Enriched GO terms of genes upregulated in the BA+NAC group compared with the BA group for plasma cells. Colour represents the \log_{10} -transformed p adjusted value. (E) UMAP plot showing 75,933 cells of 14 T cell subsets, coloured by cell type. (F) Expression of marker genes of each T cell subset. (G) Cytokine, cytotoxicity, and chemotaxis scores of

decreased after culture with NAC, and the by-product of OXPHOS mitochondrial superoxide was also reduced, as determined by MitoSOX staining and ROS detection (Fig. 3H). In addition, detecting mitochondrial DNA oxidation with 8-OHdG and OXPHOS-related protein TOM20 showed that, with NAC inhibition, the level of mitochondrial oxidative DNA decreased significantly (Fig. 3I). These findings confirmed the downregulated pathways identified in GSEA, indicating that NAC suppresses hepatic immature neutrophil respiration and OXPHOS, thus reducing ROS production.

In summary, two hepatic neutrophil subsets were defined; in addition, CD177⁺ hepatic immature neutrophils with a higher level of OXPHOS and ROS production that could be suppressed by NAC treatment were identified.

NAC treatment alleviated monocyte-mediated inflammation in liver

Monocyte-macrophage subsets (Fig. 4A) are another major component of the innate immune system; thus, we further investigated their expression and the effect of NAC treatment on that expression. Comparison of DEGs between monocyte-macrophage subsets revealed that proinflammatory, chemokine, inflammasome, and apoptosis-related genes were highly expressed in monocyte subsets (Fig. 4B), suggesting their proinflammatory role in excessive chronic liver inflammation in BA, which was also characterised by high proinflammatory¹² and inflammatory response (Hallmark) scores (Fig. 4C). In addition, Mo_CD14 and Mo-like_CD14 comprised 20.4% and 38.0% of monocyte-macrophage subsets, respectively (Fig. S5A), suggesting their main role in monocyte-mediated inflammation. In addition, the BA+NAC group exhibited higher proportions of Mo_CD14 and Mo-like_CD14 compared with the BA group (Fig. 4D).

To dissect the transcriptional differences between the BA+NAC and BA groups, DEG analysis of Mo_CD14 showed that proinflammatory, chemokine, and IFN-response genes were downregulated in the BA+NAC group (Fig. 4E and Table S5). Further GSEA was performed with gene sets from the GO, Kyoto Encyclopedia of Genes and Genomes (KEGG), and Hallmark pathways in the BA+NAC group compared with the BA group and revealed that numerous proinflammatory pathways were significantly downregulated (Fig. 4F and Table S6). In addition, DEG analysis and GSEA were performed for Mo-like_CD14. Proinflammatory, chemokine, and IFN-response genes were also downregulated in the BA+NAC group (Fig. 4G and Table S5). GSEA revealed that proinflammatory pathways were also significantly downregulated in the BA+NAC group (Fig. 4H and Table S6). However, although the Mo-like_CD14CD16 and Mo-like_CD16 subsets accounted for a minor proportion (15.7% and 11.4%, respectively) of the monocyte-macrophage subsets (Fig. S5A) and showed insignificant changes (Fig. S5B), DEG analysis and GSEA also showed that the most significantly downregulated genes and pathways in the BA+NAC group were proinflammatory and chemotaxis related (Fig. S5C-F and Tables S5 and S6).

DEG analysis and GSEA of monocyte subsets between the BA+NAC and Cont. group showed that proinflammatory,

chemotaxis-related, and lymphocyte regulatory genes and pathways were downregulated in the BA+NAC group (Fig. S6A-D and Table S5), illustrating that monocyte-mediated inflammation in BA was reduced by NAC to an even lower level than that in the Cont. group. Taken together, these results suggested that the proinflammatory function of the hepatic monocyte subsets is alleviated by NAC treatment.

NAC treatment induced hepatic macrophage polarisation and increased phagocytic function

Proportions of both TREM2⁺ macrophages and MARCO⁺ Kupffer-like macrophages were significantly decreased among all monocyte-macrophage subsets in the BA+NAC group compared with those of the BA group, but there were no significant differences compared with the Cont. group (Fig. 5A). Thus, hepatic macrophage subsets were extracted for detailed investigation.

Mac_TREM2 expressed apolipoprotein genes and class II HLA molecules, suggesting capacities of lipid metabolism and antigen presentation in this cluster. Mac_MARCO expressed complement C1Q genes and scavenger receptors, suggesting capacities of phagocytosis and innate antimicrobial immune response. However, both Mac_TREM2 and Mac_MARCO had a low expression of inflammation-related genes, indicating their M2 phenotype (Fig. 4B). These two subsets were also characterised by a high M2 and a low M1 signature score¹³ (Fig. S7A). Transcriptional differences between the BA+NAC and BA groups showed that numerous proinflammatory genes were upregulated in both macrophage subsets (Fig. S7B,C and Table S7). GSEA revealed that proinflammatory pathways were significantly upregulated in the BA+NAC group, implicating enhanced inflammatory function in hepatic macrophages (Fig. 5B,C and Table S8).

For Mac_TREM2, the peroxisome pathway was downregulated in the BA+NAC group compared with the BA group (Fig. 5B). Peroxisomes, which are multipurpose organelles in both catabolic and anabolic pathways, have important roles in lipid metabolism, ether-phospholipid biosynthesis, and ROS metabolism.¹⁴ The downregulated peroxisome pathway suggested that NAC suppresses lipid metabolism and ROS production via the peroxisome pathway in TREM2⁺ macrophages. For Mac_MARCO, the OXPHOS, *N*-acetylglucosamine metabolism, amino sugar catabolic process, and glucosamine-containing compound metabolic process pathways were downregulated in the BA+NAC group compared with the BA group (Fig. 5C). *N*-acetylglucosamine, an amino sugar, has diverse roles in different biological processes, including the modification of proteins.¹⁵ It can be converted to uridine diphosphate *N*-acetylglucosamine and, interestingly, the latter was recently reported to be reduced upon inhibition of OXPHOS,¹⁶ which is consistent with our findings. Moreover, DEG analysis and GSEA of macrophage subsets between the BA+NAC and Cont. groups showed that both Mac_TREM2 and Mac_MARCO had an enhanced inflammatory function and that Mac_MARCO had lower levels of OXPHOS, tricarboxylic acid cycle, and peroxisome metabolism processes compared with Mac_TREM2 (Fig. S7E,F and Table S7).

Kupffer cells have been reported to have decreased inflammatory and phagocytic function in BA,⁵ implying an M2-like phenotype, which was consistent with our GSEA results

cTh1, memory CD8, effector CD8, CD160⁺ CD8, Prolif CD8, $\gamma\delta$ T₁, $\gamma\delta$ T₂, and MAIT across groups. Data analysed using a 2-sided Wilcoxon rank-sum test (C.G): **p* <0.05, ***p* <0.01, ****p* <0.001. BA, biliary atresia; Cont., control; HSC, hematopoietic stem cell; MAIT, mucosal-associated invariant T cell; NAC, *N*-acetylcysteine; UMAP, uniform manifold approximation and projection.

(Fig. 4B and Fig. S7A). However, hepatic macrophages had increased inflammatory function after NAC intervention (Fig. 5B,C). Functional scores examined in Mac_MARCO showed that proinflammatory,¹² phagocytosis (GO: 0006909), inflammation response (Hallmark), and M1 scores significantly increased, whereas M2 scores significantly decreased in the BA+NAC group compared with the BA group, implying an M1-like phenotype (Fig. S7D). Subsequently, the expression levels of M1-related genes (*IRF1*, *CD86*, and *HIF1A*), proinflammatory genes (*IL1B*, *TNF*, *JUNB*, *FOSB*, and *PDE4B*), and scavenger genes (*C1QA* and *CD5L*) in Mac_MARCO were found to be significantly elevated in the BA+NAC group compared with the BA group (Fig. 5D).

To validate the downregulation of macrophage OXPHOS in the NAC+BA group, multiplex immunohistochemistry was conducted

to detect TOM20 and CD68 in liver biopsy slides. The results revealed a significant decrease in the colocalisation of TOM20 and CD68 in the BA+NAC group (Fig. 5E). This finding indicates that NAC treatment effectively inhibits OXPHOS in macrophages. In conclusion, NAC treatment suppressed hepatic macrophage OXPHOS and ROS production and reversed hepatic macrophage dysfunction by driving M1 polarisation.

Enhancement of humoral immune responses and attenuation of cellular immune responses

The adaptive immune responses, both humoral and cellular, of patients in the BA+NAC group were assessed and compared with those in the BA and Cont. groups. In total, eight B cell subsets (Fig. 6A) were identified based on known canonical marker

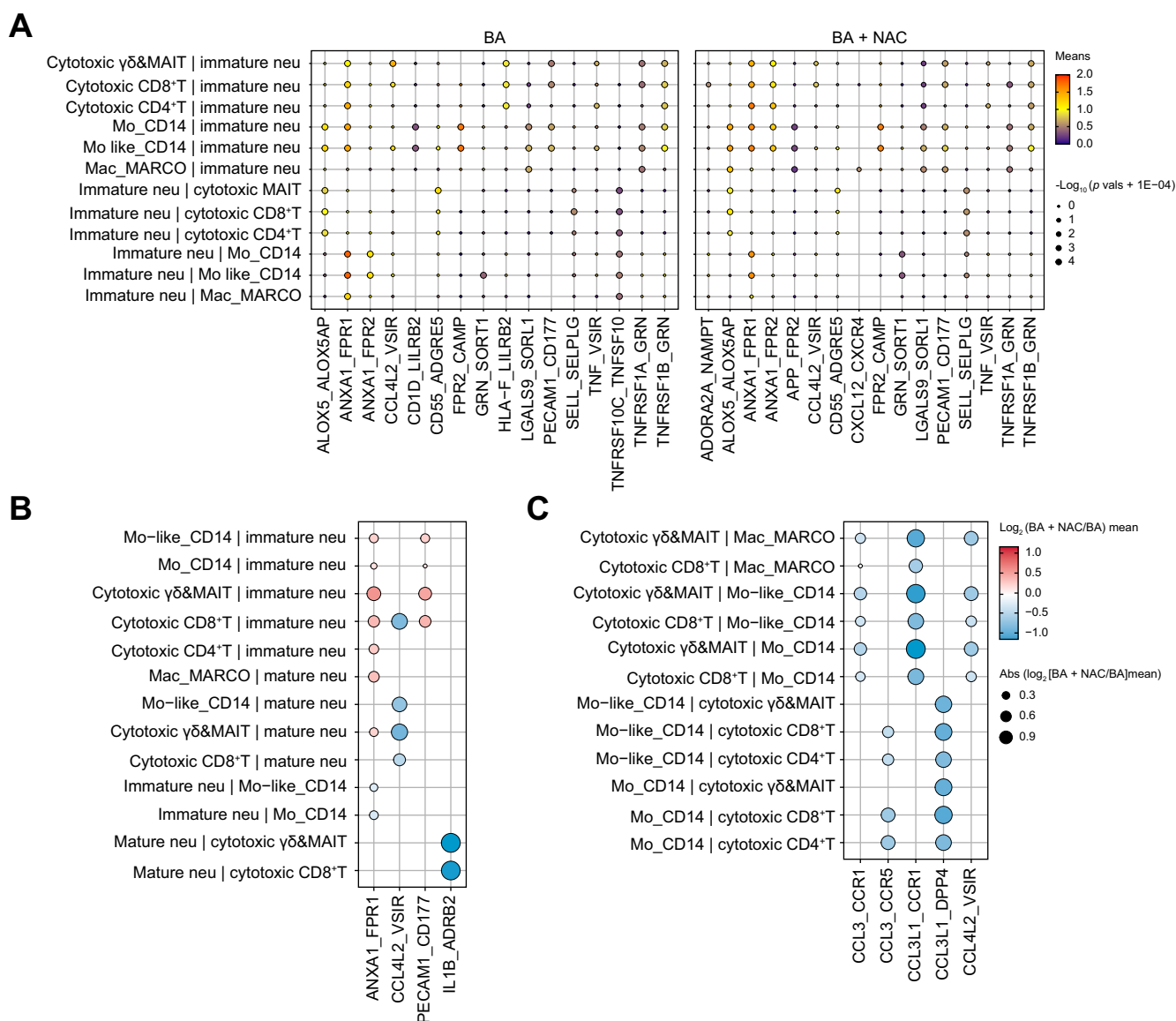


Fig. 7. Regulation of interactions between innate and lymphoid cells by NAC treatment. (A) Significant ligand–receptor pairs involved in the interaction between immature neutrophils and other immune cell subsets in the BA+NAC and BA groups; (B) selected significantly changed ligand–receptor pairs involved in the interaction between immature neutrophils and other immune cell subsets in the BA+NAC group compared with the BA group; and (C) selected significantly changed ligand–receptor pairs involved in the interaction between monocyte–macrophage subsets and lymphoid cell subsets in the BA+NAC group compared with the BA group. BA, biliary atresia; MAIT, mucosal-associated invariant T cell; NAC, N-acetylcysteine.

genes (Fig. 6B), and one abnormal subset of Doublets (Fig. S7A) was removed in downstream analysis.

The distribution of eight B cell subsets across batches and groups was visualised (Fig. S7B), and the proportions of plasma cells of all B cell subsets were found to be significantly increased in the BA+NAC group compared with the BA group, whereas there were few plasma cells in the Cont. group (Fig. 6C), suggesting that NAC treatment enhances humoral immune responses. Furthermore, gene enrichment analysis showed that upregulated DEGs were mainly enriched in the GO terms phagocytosis, humoral immune response, immunoglobulin-mediated immune responses, and antigen binding (Fig. 6D). Together, these findings suggested that NAC treatment promotes humoral immune responses elicited in BA.

In addition, 14 T cell subsets were identified based on known canonical marker genes (Fig. 6E,F), and an abnormal subset of Doublets (Fig. S7C) was removed in downstream analysis. Given that there was no significant variation in T cell subsets distribution across groups (Fig. S7D), we focussed on the transcriptional and functional analysis of T cells. Given the high expression of cytotoxic genes (Fig. S7E), the cytokine, cytotoxicity, and chemotaxis functional scores of cTh1, memory CD8, effector CD8, CD160⁺ CD8, $\gamma\delta$ T, and mucosal-associated invariant T cell (MAIT) subsets were examined; all were significantly reduced in the BA+NAC group compared with the BA and Cont. groups (Fig. 6G). Thus, overall, NAC treatment could attenuate T cell-mediated cytotoxic immune responses and proinflammatory function.

Interaction between innate and lymphoid cells

CellPhoneDB was utilised to infer the alterations in the interactions among these immune cells. First, given the heterogeneity of immature neutrophils between the BA+NAC and BA groups, we assessed the interactions between immature neutrophils and other innate/lymphoid cells (Fig. 7A). Although most interactions were shared between the BA+NAC and BA groups, several unique ligand–receptor pairs, including HLA-F/leukocyte immunoglobulin-like receptor (LILR) B2 and CD1D/LILRB2 in the BA group and CXCL12/CXCR4 in the BA+NAC group, were observed. LILRB2, also known as immunoglobulin-like transcript 4 inhibitory receptor, is upregulated on the surface with granule exocytosis after stimulation in neutrophils. Baudhuin *et al.* demonstrated that crosslinking of LILRB2 with non-classical human leukocyte antigen I molecules suppresses degranulation and phagocytosis by neutrophils, leading to neutrophil dysfunction.¹⁷ Furthermore, LILRB2 was reported to be able to inhibit CD1d antigen presentation in natural killer T cells.¹⁸ Therefore, immature neutrophils might affect lipid antigens presented by CD1d molecules in CD14⁺ monocytes. Notably, CXCL12/CXCR4, a chemokine axis reported to be involved in the retention of neutrophils within the bone marrow,¹⁹ significantly interacted between Kupffer-like macrophages and immature neutrophils in the BA+NAC group, suggesting that NAC intervention suppresses ROS-producing immature neutrophil mobilisation from bone marrow to the liver.

To further explore the regulation of interactions of the aforementioned immune cells between the BA+NAC and BA groups by NAC treatment, we selected the significantly changed ligand–receptor pairs (Fig. 7B). For neutrophils and other innate/lymphoid cells, the chemokine–receptor interaction of CCL4L2/V5IR, involved in cytokine storms as soluble mediators,²⁰ was downregulated in the BA+NAC group compared with the BA

group. CD14⁺ monocytes and cytotoxic T cells were more prone to utilise the ligand–receptor pair PECAM1/CD177 in the BA+NAC group than in the BA group, resulting in attenuation of neutrophil activation.²¹ This suggests that NAC treatment suppresses neutrophil activation via enhancement of PECAM1/CD177. In addition, both CD14⁺ monocytes and cytotoxic T cells had an increased interaction of Annexin A1 (ANXA1)/FPR1 in the BA+NAC group. ANXA1 is an important glucocorticoid-regulated protein that can limit neutrophil recruitment and the production of proinflammatory mediators.²² By targeting ANXA1/FPR1, NAC might downregulate neutrophil-mediated inflammation. Notably, β 2-adrenergic receptor (ADRB2) is a member of the superfamily of G-protein-coupled receptors and its activation is reported to lead to increased inflammatory cytokine secretion of CD8⁺ T cells.²³ It is suggested that NAC downregulates the inflammatory cytokine secretion of cytotoxic CD8⁺ T cells in the liver through decreased activation of the IL1B/ADRB2 interaction in the BA+NAC group.

In the monocyte–macrophage subsets and lymphoid cells, expression of proinflammatory chemokines, including CCL3, CCL4, CCL4L2, and their respective receptors, was decreased in the BA+NAC group compared with the BA group, indicating the potential of reducing the recruitment of these proinflammatory and cytotoxic immune cells by NAC treatment (Fig. 7C). Collectively, these findings demonstrate the potential downregulation of innate/adaptive proinflammatory responses via cell–cell interactions in BA by NAC treatment.

Discussion

In this study, we generated a clinical follow-up study and a comprehensive liver immune landscape at a single cell resolution of the response to NAC treatment in infants with BA. The findings provide further insight into alterations of various immune cell types, especially directed targeting of innate cells, by NAC treatment. BEC is a preferred target of inflammatory and immune injury to the liver.²⁴ Stimulation of innate immune responses to prolonged exogenous or endogenous insults generates an inflammatory reaction that can self-sustain and perpetuate as a result of the activation of adaptive immune mechanisms,²⁵ which is coordinated with BA pathogenesis. Collectively, the improvement in acid flow might benefit from intravenous NAC treatment through interruption of hyperinflammation resulting from the over response of the innate immune system and activation of the adaptive immune system in BA pathology after Kasai surgery.

Recent studies indicated that immature neutrophils have a crucial role in inflammatory processes, such as systemic vascular inflammation²⁶ or coronavirus disease 2019 (COVID-19²⁷) via NET release. Our previous study also showed that CD177⁺ neutrophils cause BEC damage by increasing OXPPOS and ROS levels.⁸ According to our scRNA-seq and experimental data, NAC treatment suppressed the downregulation of CD177⁺ immature neutrophil proinflammatory function by suppressing OXPPOS, ROS production, and NET release as innate immune responses, highlighting the direct effects on innate cells. Interestingly, the OXPPOS levels of immature neutrophils in the BA+NAC group were even lower than those in the Cont. group, indicating strong antioxidant effects of NAC. Additionally, although the OXPPOS levels of mature neutrophils were not directly affected, NAC appeared to suppress the innate immune responses of mature

neutrophils; however, the details of the mechanism involved require further exploration.

Monocytes and macrophages have central roles in the initiation and resolution of inflammation in the innate immune system.²⁸ CD14⁺ monocytes have been considered to induce monocyte-centric inflammatory storms in severe COVID-19, which can be suppressed by the immunosuppressive agent tocilizumab.²⁹ Based on our data, four monocyte subsets were identified in response to inflammation; proinflammatory function was significantly downregulated in the BA+NAC group compared with both the BA and Cont. groups, suggesting that NAC suppresses the proinflammatory responses triggered by monocytes.

However, hypoinflammatory hepatic macrophages appeared to exhibit enhanced phagocytic and inflammatory functions and induced M1 polarisation following NAC intervention. Kupffer cell dysfunction, characterised by decreased phagocytic and inflammatory function in BA,⁵ was reversed by NAC treatment. Proinflammatory M1 macrophages rely mainly on glycolysis and exhibit impairment of the tricarboxylic acid cycle, whereas anti-inflammatory M2 macrophages are more dependent on mitochondrial OXPHOS.³⁰ NAC has also been reported to stimulate inflammatory gene expression in peripheral blood mononuclear cell cultures,³¹ which supports our findings. The suppression of OXPHOS in Kupffer cells might drive M1 polarisation, although the mechanism involved requires further investigation.

In addition, plasma cells were upregulated after NAC treatment. The increase in autoantibodies in patients with BA³² might be directly related to the functional dysregulation of B cells.^{8,33} The detailed function of plasma cells in terms of antibody production and BEC damage regulated by NAC still needs further elucidation. Additionally, the attenuation of cellular immune responses might be associated with the suppression of innate immune responses, given that interactions via chemokines/receptors between innate cells and lymphoid cells were significantly decreased. Unexpectedly, interactions involved in immune dysfunction and pathogenic immature neutrophil mobilisation were downregulated, emphasising the potential benefits of NAC. However, the recently reported fibrosis-related interactive pairs in BA³⁴ were not significantly altered in the BA+NAC groups, indicating that NAC might not affect liver fibrosis.

In conclusion, despite the limitations of a lack of hepatocytes and CD45⁻ non-parenchymal cells and a small sample size, our data present deeper insights into the regulation of liver immune function by intravenous NAC treatment in infants with BA at a single cell resolution. The data showed that NAC partially reverses liver immune dysfunction and alleviates the proinflammatory responses in BA mainly by targeting innate cells. This study also provides evidence for the beneficial response of BA to NAC therapeutic strategies although further large-scale clinical trials will be required to progress this treatment approach.

Abbreviations

ADRB2, β 2-adrenergic receptor; ALP, alkaline phosphatase; ANXA1, Annexin A1; BA, biliary atresia; BEC, biliary epithelial cell; COVID-19, coronavirus 2019; DBIL, direct bilirubin; DEGs, differentially expressed genes; GO, Gene Ontology; GSEA, gene set enrichment analysis; HSC, haematopoietic stem cell; IBIL, indirect bilirubin; IFN, interferon; LILR, leukocyte immunoglobulin-like receptor; ILC, innate lymphoid cell; KEGG, Kyoto Encyclopedia of Genes and Genomes; MAIT, mucosal-associated invariant T cell; MFI, mean fluorescence intensity; MHC, major histocompatibility complex; NAC, N-acetylcysteine; NES, normalised enrichment score; NETs, neutrophil extracellular traps; OXPHOS, oxidative phosphorylation; pDC, plasmacytoid dendritic cell; ROS, reactive oxygen species; scRNA-seq, single cell RNA-sequencing; TBIL, total bilirubin; UMAP, uniform manifold approximation and projection; UMI, unique molecular identifier.

Financial support

This study was supported by funds from National Natural Science Foundation of China (81974056 and 82271750), Science and Technology Planning Project of Guangdong Province (2019B020227001), and Science and Technology Planning Project of Guangzhou (2023B03J1299 and 202206080002).

Conflicts of interest

The authors declare no conflicts of interest that pertain to this work.

Please refer to the accompanying ICMJE disclosure forms for further details.

Authors' contributions

Performed the experiments: RY, SM, JS, LT, LS, YT, HC, MF, ZZ, GZ. Recruited patients, provided clinical information, and performed clinical care: JY, WZ, JZ, FL, CC, ZW, XG, TL, JL, HS. Performed bioinformatic and statistical analysis: RY, XZ, YZ. Wrote the manuscript: RY, YC, SM. Conceived and supervised the project: ZW, RZ, HX.

Data availability statement

Further information and requests for resources and reagents should be directed to the lead contact, Ruizhong Zhang. The raw sequencing data that support the findings of this study were deposited into the Genome Sequence Archive of Beijing Institute of Genomics, Chinese Academy of Sciences: CODE (BF2021060306447), website (in pending). For data access, please follow the guidelines of the Genome Sequence Archive (<http://bigd.big.ac.cn/gsa-human>). Publicly available software is specified in the supplementary data online, and the key resources are shown in the CTAT table in the supplementary data online.

Acknowledgements

The authors thank the Clinical Biological Resource Bank of Guangzhou Women and Children's Medical Center for providing the clinical samples. The authors thank Jianming Zeng and all members of his bioinformatics team, Biotrainee, for generously sharing their experience and codes, and Jun Zhang for generously sharing his skills and codes of bioinformatic visualisation. The authors also thank the team of the Annoroad Gene Company for support with single cell sequencing. The pilot study of NAC treatment in patients with BA is registered on the Chinese Clinical Trial Registry (ChiCTR2000040505).

Supplementary data

Supplementary data to this article can be found online at <https://doi.org/10.1016/j.jhepr.2023.100908>.

References

Author names in bold designate shared co-first authorship

- [1] **Japanese Biliary Atresia Society, Nio M, Muraji T.** Multicenter randomized trial of postoperative corticosteroid therapy for biliary atresia. *Pediatr Surg Int* 2013;29:1091–1095.
- [2] **Kim S, Moore J, Alonso E, Bednarek J, Bezerra JA, Goodhue C, et al.** Correlation of immune markers with outcomes in biliary atresia

- following intravenous immunoglobulin therapy. *Hepatol Commun* 2019;3:685–696.
- [3] Baumann U, Sturm E, Lacaille F, Gonzalès E, Arnell H, Fischler B, et al. Effects of odevixibat on pruritus and bile acids in children with cholestatic liver disease: phase 2 study. *Clin Res Hepatol Gastroenterol* 2021;45:101751.
- [4] Nguyen HPA, Ren J, Butler M, Li H, Qazi S, Sadiq K, et al. Study protocol of Phase 2 open-label multicenter randomized controlled trial for granulocyte-colony stimulating factor (G-CSF) in post-Kasai Type 3 biliary atresia. *Pediatr Surg Int* 2022;38:1019–1030.
- [5] Wang J, Xu Y, Chen Z, Liang J, Lin Z, Liang H, et al. Liver immune profiling reveals pathogenesis and therapeutics for biliary atresia. *Cell* 2020;183:1867–1883.
- [6] Chiew AL, Isbister GK, Kirby KA, Page CB, Chan BSH, Buckley NA, et al. Massive paracetamol overdose: an observational study of the effect of activated charcoal and increased acetylcysteine dose (ATOM-2). *Clin Toxicol (Phila)* 2017;55:1055–1065.
- [7] Hu J, Zhang Q, Ren X, Sun Z, Quan Q. Efficacy and safety of acetylcysteine in "non-acetaminophen" acute liver failure: a meta-analysis of prospective clinical trials. *Clin Res Hepatol Gastroenterol* 2015;39:594–599.
- [8] Zhang R, Su L, Fu M, Wang Z, Tan L, Chen H, et al. CD177+ cells produce neutrophil extracellular traps that promote biliary atresia. *J Hepatol* 2022;77:1299–1310.
- [9] Luo Z, Shivakumar P, Mourya R, Gutta S, Bezerra JA. Gene expression signatures associated with survival times of pediatric patients with biliary atresia identify potential therapeutic agents. *Gastroenterology* 2019;157:1138–1152.
- [10] Schulte-Schrepping J, Reusch N, Paclik D, Baßler K, Schlickeiser S, Zhang B, et al. Severe COVID-19 is marked by a dysregulated myeloid cell compartment. *Cell* 2020;182:1419–1440.
- [11] Evrard M, Kwok IWH, Chong SZ, Teng KWW, Becht E, Chen J, et al. Developmental analysis of bone marrow neutrophils reveals populations specialized in expansion, trafficking, and effector functions. *Immunity* 2018;48:364–379.
- [12] Aizarani N, Saviano A, Sagar, Maily L, Durand S, Herman JS. A human liver cell atlas reveals heterogeneity and epithelial progenitors. *Nature* 2019;572:199–204.
- [13] Long Z, Sun C, Tang M, Wang Y, Ma J, Yu J, et al. Single-cell multiomics analysis reveals regulatory programs in clear cell renal cell carcinoma. *Cell Discov* 2022;8:68.
- [14] Jo DS, Cho DH. Peroxisomal dysfunction in neurodegenerative diseases. *Arch Pharm Res* 2019;42:393–406.
- [15] Ansari S, Kumar V, Bhatt DN, Irfan M, Datta A. N-acetylglucosamine sensing and metabolic engineering for attenuating human and plant pathogens. *Bioengineering (Basel)* 2022;9:64.
- [16] Cao J, Li M, Liu K, Shi X, Sui N, Yao Y, et al. Oxidative phosphorylation safeguards pluripotency via UDP-N-acetylglucosamine. *Protein Cell* 2023;14:376–381.
- [17] Baudhuin J, Migraine J, Faivre V, Loumagne L, Lukaszewicz AC, Payen D, et al. Exocytosis acts as a modulator of the ILT4-mediated inhibition of neutrophil functions. *Proc Natl Acad Sci U S A* 2013;110:17957–17962.
- [18] Li D, Wang L, Yu L, Freundt EC, Jin B, Screaton GR, et al. Ig-like transcript 4 inhibits lipid antigen presentation through direct CD1d interaction. *J Immunol* 2009;182:1033–1040.
- [19] Martin C, Burdon PC, Bridger G, Gutierrez-Ramos JC, Williams TJ, Rankin SM. Chemokines acting via CXCR2 and CXCR4 control the release of neutrophils from the bone marrow and their return following senescence. *Immunity* 2003;19(4):583–593.
- [20] Fajgenbaum DC, June CH. Cytokine storm. *N Engl J Med* 2020;383:2255–2273.
- [21] Deng H, Hu N, Wang C, Chen M, Zhao MH. Interaction between CD177 and platelet endothelial cell adhesion molecule-1 downregulates membrane-bound proteinase-3 (PR3) expression on neutrophils and attenuates neutrophil activation induced by PR3-ANCA. *Arthritis Res Ther* 2018;20:213.
- [22] Sugimoto MA, Vago JP, Teixeira MM, Sousa LP. Annexin A1 and the resolution of inflammation: modulation of neutrophil recruitment, apoptosis, and clearance. *J Immunol Res* 2016;2016:8239258.
- [23] Slota C, Shi A, Chen G, Bevans M, Weng NP. Norepinephrine preferentially modulates memory CD8 T cell function inducing inflammatory cytokine production and reducing proliferation in response to activation. *Brain Behav Immun* 2015;46:168–179.
- [24] Strazabosco M, Fiorotto R, Cadamuro M, Spirli C, Mariotti V, Kaffe E, et al. Pathophysiologic implications of innate immunity and autoinflammation in the biliary epithelium. *Biochim Biophys Acta Mol Basis Dis* 2018;1864:1374–1379.
- [25] Szabo G, Petrasek J. Inflammasome activation and function in liver disease. *Nat Rev Gastroenterol Hepatol* 2015;12:387–400.
- [26] Wang L, Ai Z, Khojraty T, Zec K, Eames HL, van Grinsven E, et al. ROS-producing immature neutrophils in giant cell arteritis are linked to vascular pathologies. *JCI Insight* 2020;5:e139163.
- [27] Rice CM, Lewis P, Ponce-Garcia FM, Gibbs W, Groves S, Cela D, et al. Hyperactive immature state and differential CXCR2 expression of neutrophils in severe COVID-19. *Life Sci Alliance* 2022;6:e202201658.
- [28] Auffray C, Sieweke MH, Geissmann F. Blood monocytes: development, heterogeneity, and relationship with dendritic cells. *Annu Rev Immunol* 2009;27:669–692.
- [29] Guo C, Li B, Ma H, Wang X, Cai P, Yu Q, et al. Single-cell analysis of two severe COVID-19 patients reveals a monocyte-associated and tocilizumab-responding cytokine storm. *Nat Commun* 2020;11:3924.
- [30] Liu Y, Xu R, Gu H, Zhang E, Qu J, Cao W, et al. Metabolic reprogramming in macrophage responses. *Biomark Res* 2021;9:1.
- [31] Al-Shukaili A, Al-Abri S, Al-Ansari A, Monteil MA. Effect of N-acetyl-L-cysteine on cytokine production by human peripheral blood mononuclear cells. *Sultan Qaboos Univ Med J* 2009;9:70–74.
- [32] Luo Y, Brigham D, Bednarek J, Torres R, Wang D, Ahmad S, et al. Unique cholangiocyte-targeted IgM autoantibodies correlate with poor outcome in biliary atresia. *Hepatology* 2021;73:1855–1867.
- [33] Taylor SA, Assis DN, Mack CL. The contribution of B cells in autoimmune liver diseases. *Semin Liver Dis* 2019;39:422–431.
- [34] Ye C, Zhu J, Wang J, Chen D, Meng L, Zhan Y, et al. Single-cell and spatial transcriptomics reveal the fibrosis-related immune landscape of biliary atresia. *Clin Transl Med* 2022;12:e1070.